Agriculture, Ecosystems and Environment 394 (2025) 109881

Contents lists available at ScienceDirect

Agriculture, Ecosystems and Environment

journal homepage: www.elsevier.com/locate/agee

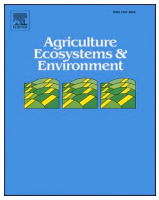

Rare rather than abundant *phoD*-harboring bacteria shape soil phosphorus bioavailability in karst orchard–medicinal plant intercropping systems

Chenggang Liu [a,*], Chuan Jiang [a,c], Xiaoling Zeng [a,c], Yuanyang Chen [a,d], Yanqiang Jin [a], Akash Tariq [e], Shujie Chen [a,c], Belayneh Azene [a], Fuzhao Huang [b,*]

[a] *CAS Key Laboratory of Tropical Plant Resources and Sustainable Use, Xishuangbanna Tropical Botanical Garden, Chinese Academy of Sciences, Menglun 666303, China*

[b] *Guangxi Key Laboratory of Plant Conservation and Restoration Ecology in Karst Terrain, Guangxi Institute of Botany, Guangxi Zhuang Autonomous Region and Chinese Academy of Sciences/Guangxi Guilin Urban Ecosystem National Observation and Research Station, Guilin 541006, China*

[c] *University of Chinese Academy of Sciences, Beijing 100049, China*

[d] *School of Agriculture, Yunnan University, Kunming 650504, China*

[e] *Xinjiang Key Laboratory of Desert Plant Roots Ecology and Vegetation Restoration, Xinjiang Institute of Ecology and Geography, Chinese Academy of Sciences, Urumqi 830011, China*

ARTICLE INFO

Keywords:
Alkaline phosphatase
Ecological restoration
Karst region
Medicinal plant
Soil P bioavailability

ABSTRACT

Cultivating medicinal plants in orchards has emerged as a promising strategy to improve soil nutrient profiles, utilize under-tree space effectively, and boost farmers' incomes. However, the mechanisms influencing soil phosphorus (P) bioavailability in orchard–medicinal plant intercropping systems (OMIs) remain unclear, particularly in karst regions where P is severely deficient, and intercropping effects vary by medicinal plant species. This study assessed the short-term effects of medicinal plant intercropping on soil P bioavailability in four OMIs (*Prunus. salicina* + *Hypericum monogynum* [PH], *P. salicina* + *Polygala fallax* [PP], *P. salicina* + *Rubus suavissmus*, and *P. salicina* + *Semiliquidambar cathayensis* + *Illicium difengpi*) in the karst region of the Lijiang River Basin, Southwest China, with *P. salicina* monoculture (Pm) as a control. Compared with Pm, OMIs generally reduced soil bioavailable P fractions, except $CaCl_2$-P, while increasing microbial biomass P, potentially enhancing temporary organic P (P_o) reserves. These changes supported plant inorganic P (P_i) uptake from the rhizosphere soil, as shown by shifts in P activation, supply capacity, and acquisition strategies. Furthermore, OMIs significantly altered the composition and structure, though not the diversity, of *phoD*-harboring bacterial communities. While abundant taxa (e.g., *Bradyrhizobium*) and rare taxa (e.g., *Pseudomonas*) responded differently to nutrient changes, rare taxa exhibited greater responsiveness, particularly in the PH and PP systems. Soil bioavailable P fractions were primarily regulated by rare *phoD*-harboring bacteria, influenced by soil N:P ratio, pH, and moisture. Overall, OMIs, particularly PH and PP, shifted P utilization strategies from P_i acquisition to temporary P_o preservation, improving P-use efficiency through plant-specific impacts on rare *phoD*-harboring bacteria. These findings highlight the importance of selecting medicinal plants for optimizing P cycling and suggest that targeted P fertilization in OMIs could enhance karst soil productivity.

1. Introduction

Forestland resources are becoming increasingly vital amid global environmental change, biodiversity loss, and natural resource depletion. Sustainable land-use strategies that simultaneously balance ecological integrity and economic viability have emerged as a critical research priority (Lu et al., 2020). One such strategy is the orchard–medicinal plant intercropping systems (OMIs), an agroforestry model that integrates perennial fruit trees with medicinal plants through spatial and temporal arrangements (Pérez-Nicolás et al., 2018; Zhang et al., 2020). This system addresses the protracted investment cycles associated with tree cultivation and the inefficient utilization of forest resources. By optimizing land productivity through vertical stratification and complementary resource use (Deng et al., 2023), OMIs offer a promising solution to reconcile ecological conservation with economic development, particularly in the context of sustainable forestry and traditional

* Corresponding authors.
E-mail addresses: liuchenggang@xtbg.ac.cn (C. Liu), fuzhaoh@gxib.cn (F. Huang).

https://doi.org/10.1016/j.agee.2025.109881
Received 11 December 2024; Received in revised form 9 July 2025; Accepted 23 July 2025
Available online 25 July 2025

medicinal plant production (Chen et al., 2016). While existing research has examined various aspects of OMIs, including medicinal plants adaptation (Applequist et al., 2020), yield and bioactive compounds (Wang et al., 2021), and basic soil characteristics (Zhang et al., 2020), the mechanisms governing soil nutrient cycling in karst-derived OMIs remains insufficiently studied.

Soil phosphorus (P) is a vital macronutrient for plant growth and development, often serving as a limiting factor in intercropping productivity (Liu et al., 2021a, 2025). However, due to P inherently low mobility and high fixation capacity in soils, only 10 %–15 % of applied P fertilizers are utilized annually by plants, leading to significant economic losses and potential environmental risks (Malik et al., 2012). Soil P exists in various inorganic and organic forms, with their bioavailability governed by complex interactions among soil constituents (Liu et al., 2018). Inorganic P (P_i) predominantly associates with Fe, Al, and Ca oxides, with its solubility strongly pH-dependent (Zhang et al., 2023). Organic P (P_o), constituting 30 %–65 % of total soil P, occurs as various esters whose availability depends on microbial-mediated mineralization and decomposition (Wan et al., 2022). These dynamics are particularly pronounced in calcareous karst soils, where calcium carbonate acts as primary P adsorption substrate, reducing P_i availability to < 5 % of total P and thereby making P_o mineralization crucial for plant nutrition (Dong et al., 2024; Tian et al., 2022).

Microorganisms play critical roles in soil P cycling by secreting extracellular enzymes, with alkaline phosphatase (ALP) being particularly important for P_o mineralization under P-limited conditions (Wei et al., 2019). In intercropping systems, ALP originates mainly from microorganisms, particularly bacteria (Spohn and Kuzyakov, 2013), and drives microbial P turnover, mineralizing 90 % of soil P_o compounds except phytates (Roy et al., 2025). Microbial ALP is encoded by three homologous genes (*phoA*, *phoD*, and *phoX*) (Chen et al., 2023), among which *phoD* demonstrates both ubiquity across soil types and responsiveness to P deficiency (Fraser et al., 2015; Wei et al., 2021). The composition and activity of abundant and rare *phoD*-harboring bacterial communities are susceptible to land-use practices such as intercropping and fertilization regimes (Dai et al., 2020; Xie et al., 2020). In karst regions, these microbial processes are further constrained by high rock exposure and shallow soils (Li et al., 2025; Zeng et al., 2024), which collectively exacerbate the challenge of enhancing P availability during OMIs implementation.

Intercropping systems exert a significant influence on soil P availability by facilitating complex plant-microbe synergistic interactions, thereby enhancing P acquisition efficiency. These systems leverage complementary ecological niches to activate multiple P-mobilization pathways simultaneously: 1) root-mycorrhizal networks amplify *phoD*-harboring bacterial activity in the rhizosphere to capture labile P_i (Spohn and Kuzyakov, 2013); 2) organic acids exudates (e.g., citrate and malate) not only solubilize active P_i but also stimulate ALP-producing microbes (Liu et al., 2025); 3) Plant-derived phosphatases complement microbial ALP in hydrolyzing unstable P_o (Dong et al., 2024); and 4) more root-mediated proton secretion to mobilize occluded P (DeLuca et al., 2015). Although such synergies have been widely studied in conventional agroforestry systems (Liu et al., 2018; Wang et al., 2023a), OMIs exhibit unique dynamics mainly due to the release of secondary metabolites from medicinal plant roots, which influence microbial community composition and activity. Therefore, current understanding of the impacts of OMIs construction on soil P forms and availability and the regulatory role of microorganisms remains limited and require further investigation.

The Lijiang River Basin in northeastern Guangxi Province is globally renowned for its unique karst landforms. In March 2018, Guilin was designated as an innovation demonstration zone under the National Sustainable Development Agenda to protect the ecological environment of the Lijiang River Basin. Despite these efforts, rocky desertification remains a persistent issue, necessitating urgent vegetation restoration to address the fragile karst ecosystem (Guo et al., 2022; Li et al., 2025). Recent experiments have identified leguminous species and models such as *Zenia insignis*, *Leucaena leucocephala*, and *Chamaecrista rotundifolia* for vegetation restoration in rocky desertified areas (Cheng et al., 2022; Guo et al., 2022). However, the effectiveness of these models is constrained by degraded soils and underused understory spaces (Dong et al., 2024). Thus, establishing OMIs is crucial for addressing ecological and economic challenges by enhancing P availability via microbial-mediated processes in this karst region.

This study investigated the short-term effects of intercropping various medicinal plants on soil P availability and microbial P-regulation mechanisms in typical OMIs established on P-deficient soils of the karst region in Southwest China's Lijiang River Basin. The research assessed P bioavailability, *phoD*-harboring bacterial communities, and other soil physicochemical properties. The study focused on the following hypotheses: i) OMIs enhance soil P bioavailability by promoting plant uptake and stimulating P-mobilizing bacterial communities (*phoD* gene communities); ii) soil pH, influenced by karst calcium carbonate, plays a key role in P cycling; and iii) the *phoD* gene communities positively affects P availability. Findings are intended to support ecological restoration, foster regional economic development in the Lijiang River karst region, and aid in conserving rare and endangered medicinal plants.

2. Materials and methods

2.1. Site description

The study was conducted in the Guanyan subterranean river basin, part of the middle reaches of the Lijiang River in Guangxi, Southwest China (25°01'–25°16'N, 110°27'–110°37'E; 880–950 m a.s.l.), a region characterized by typical karst landscapes. The area has a subtropical monsoon climate, with a mean annual temperature of 17.8 °C, precipitation of 1950 mm, 1243 h of sunshine, and a frost-free period of approximately 300 days. The soil is brown calcareous, characterized by high gravel content, coarse texture, and shallow layers, leading to severe erosion. Over the past decade, rapid economic and social development in the Guanyan Basin has led to widespread vegetation degradation. Large-scale replacement of natural slope vegetation with *Prunus salicina* orchard plantations has simplified vegetation structures, reduced carbon sink capacity, increased soil and water loss, and exacerbated rocky desertification.

2.2. Experimental design and soil collection

To address the above issues, *P. salicina*–based OMIs were established in early 2020. *P. salicina* trees, planted at 3 m × 4 m spacing in 2010, have now reached maturity. Two-year-old bagged Chinese medicinal seedlings were interplanted between two *P. salicina* trees at diagonal crossings with 1.5 m × 2.0 m spacing. The uniform management practice was implemented without the addition of any supplemental fertilizers subsequent to the initial base fertilization. The OMIs included four combinations: *P. salicina* + *Hypericum monogynum* (PH), *P. salicina* + *Polygala fallax* (PP), *P. salicina* + *Rubus suavissmus* (PR), and *P. salicina* + *Semiliquidambar cathayensis* + *Illicium difengpi* (PSI). *P. salicina* monoculture (Pm) served as the control. Each treatment featured three 20 m × 20 m replicate plots with a 100-m buffer zone. Plots were further divided into three blocks. In September 2022 (growing season), 15 random topsoil (0–20 cm) cores per block were collected using a 5-cm soil auger after removing surface litter to avoid the variation of karst soils. Cores were combined into composite samples, immediately transported on ice, and manually cleaned of visible stones, plant, and animal debris. Each block yielded three composite samples, resulting in 45 samples across the five OMIs. Samples were sieved through a 2-mm mesh and divided into three subsamples for biochemical and molecular analyses.

2.3. Soil characteristics analysis

Soil moisture was measured gravimetrically and expressed as a percentage of dry weight. Soil pH was determined in a 1: 2.5 soil-to-water mixture using a digital pH meter (FE28; Mettler Toledo, USA). Total carbon (TC) and total nitrogen (TN) were quantified via dry combustion using an elemental analyzer (Vario MAX CN; Elementar, Germany). Total P (TP) was digested with $HClO_4$–HF and measured via inductively coupled plasma atomic emission spectrometry (ICP-AES, iCAP6300; Thermo Fisher, USA). Available P (AP) was extracted with 0.03 M NH_4F–0.025 M HCl and analyzed with a segmented flow analyzer (Auto Analyzer 3; SEAL Analytical GmbH, Germany). ALP activity was determined using 0.5 % disodium phenyl phosphate as a substrate and defined as phenol released in 1 h per gram of soil (Wang et al., 2022). Microbial biomass P (MBP) was extracted with 0.5 M $NaHCO_3$ and calculated as the difference between fumigated and unfumigated soils divided by a correction factor 0.4 (Liu et al., 2021a). The TC, TN, and TP contents in plant leaves and roots were analyzed using the protocol described by Liu et al. (2019).

2.4. P fractionation via biologically-based method

Soil P was fractionated using the modified biologically-based P (BBP) method to evaluate plant P acquisition strategies and bioavailability across complex landscapes (DeLuca et al., 2015). Fresh soil was extracted in parallel with 10 mM $CaCl_2$, 10 mM citric acid, 0.02 enzyme unit extract, and 1 M HCl, followed by 3 h of shaking at 200 rpm. Extracted soil was filtered through a 0.45 μm Whatman No. 42 membrane, and the P concentration in the supernatant was measured using ICP-AES (Wan et al., 2022).

2.5. phoD amplicon sequencing, sequence processing and diversity analyses

Soil DNA was extracted using the FastDNA® Spin Kit (MP Biomedicals, USA) following the manufacturer's instructions. DNA quality and concentration were assessed using 1.0 % agarose gel electrophoresis and NanoDrop2000 spectrophotometry (Thermo Fisher, USA). The *phoD* gene was amplified using the primers ALPS-733F (5′-TGGGAYGATCAYGARGT-3′) and ALPS-1083R (5′-CTGSGCSAKSACRTTCCA-3′) (Wang et al., 2022), following PCR protocols (Chen et al., 2021). Amplification products were purified with a PCR Clean-Up Kit (YuHua, China) and pair-end sequenced on an Illumina MiSeq PE300 platform (Illumina, USA) at Majorbio Bio-Pharm Technology Co. Ltd. (Shanghai, China). Raw sequencing data were demultiplexed using an in-house Perl script, quality-filtered using fast alignment search tool-all with quality, and merged with fast length adjustment of short reads (FLASH). Optimized sequences were clustered into operational taxonomic units (OTUs) at 97 % similarity using UPARSE after chimera removal. Taxonomic assignments for OTUs were performed with the ribosomal database project classifier. All datasets were restricted to equal sequencing depth for downstream analysis. Based on the relative abundances, taxa were classified as abundant (>0.1 %) and rare (<0.01 %) (Xiong and Wan, 2023). Diversity metrics, including Shannon, Chao1, and Simpson indices, were calculated using the R libraries *picante* and *vegan*. Raw reads are available in the NCBI Sequence Read Archive under accession number PRJNA1072637.

2.6. Statistical analyses

Statistical analyses were conducted in R (version 3.4.2). One-way analysis of variance (ANOVA) with Tukey's HSD test ($P < 0.05$) determined differences in soil P fractions, soil properties, and *phoD*-harboring bacterial diversity across OMIs. Redundancy analysis (RDA) assessed soil P fraction distributions among ecosystems, while nonmetric multidimensional scaling (NMDS) ordinations with Bray–Curtis distance visualized *phoD* bacterial community dissimilarity using the "*vegan*" package. Mantel tests evaluated associations between soil physicochemical properties and *phoD* bacterial communities using the "*ggcor*" and "*vegan*" package. Pearson's correlation tested relationships between *phoD* bacterial diversity, key taxa, and soil variables using the "*correlation*" package. Network analysis of interaction between P fractions and *phoD* bacteria based on Spearman's correlation coefficients was visualized with Gephi v.0.9.2.

3. Results

3.1. Soil and plant characteristics

Soil moisture significantly increased in PH, PP, and PR systems compared with Pm system (Table S1). Soil pH, TC, and TN were similar across systems, except for higher pH in PP and TN content in PH. OMIs reduced C:N ratio and increased C:P and N:P ratios compared with Pm, particularly in PH. Leaf and root TC, TN, and TP varied significantly among plant species, although root biomass did not (Table S2). Compared with Pm, PP and PR lowered average leaf TC but increased leaf TN and TP. Conversely, PH increased root TC, TN, and TP across species, while other OMIs reduced root TC and TN compared with Pm.

3.2. Soil P fractions and ALP activity

TP and ALP activity did not differ significantly between Pm and OMIs (Fig. 1a and d). PH and PP reduced AP and increased MBP relative to Pm (Fig. 1b and c). Among the OMIs, PR showed higher TP, AP, and ALP activities but lower MBP than PH (Fig. 1). $CaCl_2$-P was similar across all systems (Fig. 2a). OMIs reduced citrate-P and HCl-P compared with Pm, except for higher citrate-P in PR (Fig. 2b and d). PH alone showed reduced enzyme-P compared with Pm (Fig. 2c). PR demonstrated higher $CaCl_2$-P, enzyme-P, and citrate-P levels than other OMIs (Fig. 2b, c, and d). Except for PR, OMIs showed lower ratios of AP/TP, citrate-P/$CaCl_2$-P, HCl-P/$CaCl_2$-P, and citrate-P/enzyme-P but higher MBP/TP and MBP/AP ratios than Pm. However, ratios of enzyme-P/$CaCl_2$-P, HCl-P/citrate-P, and HCl-P/enzyme-P did not differ between Pm and OMIs (Table S3).

3.3. phoD-harboring bacterial community

Cluster analysis revealed 9839 OTUs, with 981 shared across all ecosystems (13.9 % abundant and 37.4 % rare). Among rare OTUs, 164 were shared between Pm and PH, 254 between Pm and PP, 229 between Pm and PR, and 421 between Pm and PSI (Fig. 3a). Unique OTUs were numbered 1006 for Pm, 299 for PH, 627 for PP, 809 for PR, and 1127 for PSI. Proteobacteria (13.0 %–15.1 %), Actinobacteria (7.4 %–16.0 %), Planctomycetes (6.3 %–9.9 %), and Acidobacteria (0.4 %–8.7 %) dominated the *phoD*-harboring community, with *Bradyrhizobium*, *Streptomyces*, *Planctomyces*, and *Luteitalea* as their most abundant genera (Fig. 3b and c). PH and PP had slightly higher relative abundances of Planctomycetes and Acidobacteria and lower Actinobacteria and Proteobacteria compared with Pm. Rare communities exhibited more Actinobacteria but fewer Acidobacteria and Planctomycetes. These trends were consistent across corresponding genera.

The NMDS plot showed a clear separation in the structure of the *phoD*-harboring bacterial community across systems (perMANOVA, all: $r^2 = 0.30$, $P < 0.001$; abundant: $r^2 = 0.23$, $P < 0.001$; rare: $r^2 = 0.45$, $P < 0.001$; Fig. 3d). The α-diversity of *phoD* bacteria was unaffected by OMIs, except for the abundant community (Fig. S1), with no significant differences between Pm and OMIs. Generally, the Shannon and richness indices of the abundant community in PH were higher, while the evenness index exhibited the opposite trend. Richness/$Shannon_{abundant}$ was significantly lower than richness/$Shannon_{rare}$, and both were positively correlated (Fig. S2). Richness/$Shannon_{abundant}$ explained 33.5 % and 27.8 % of the total community richness/Shannon (richness/

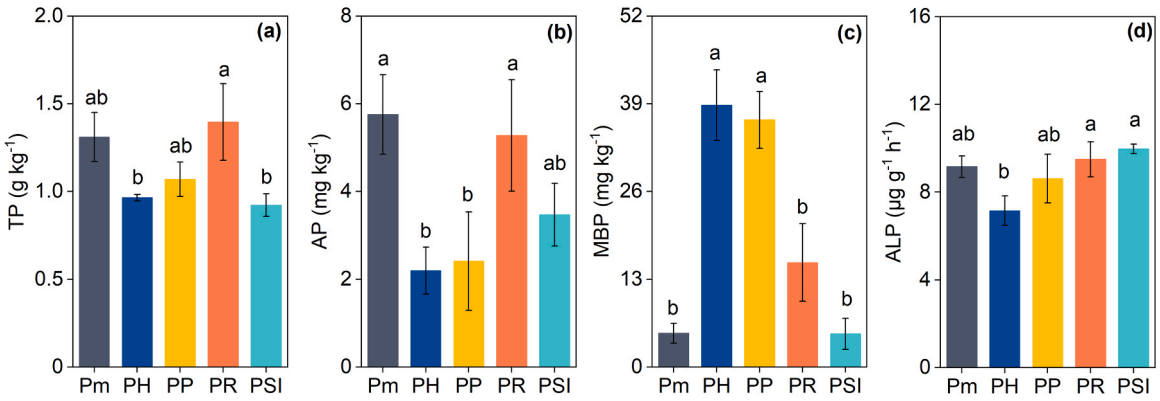

Fig. 1. Changes in soil total phosphorus (a), available phosphorus (b), microbial biomass phosphorus (c), and alkaline phosphatase activity (d) under different orchard–medicinal plant intercropping systems. Values represent means ± SEs. Different letters indicate significant differences at the $P < 0.05$ level. TP: total phosphorus; AP: available phosphorus; MBP: microbial biomass phosphorus; ALP: alkaline phosphatase activity. Pm: *Prunus salicina* monoculture; PH: *P. salicina* + *Hypericum monogynum*; PP: *P. salicina* + *Polygala fallax*; PR: *P. salicina* + *Rubus suavissmus*; PSI: *P. salicina* + *Semiliquidambar cathayensis* + *Illicium difengpi*.

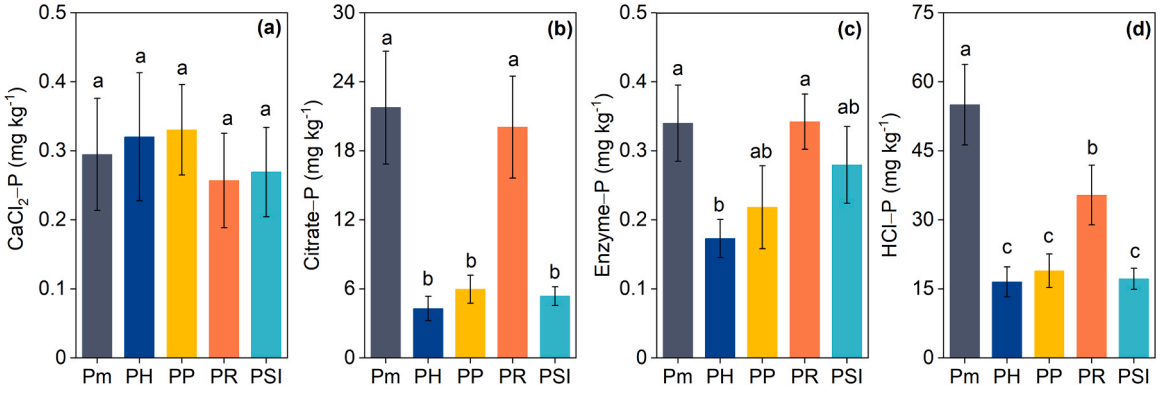

Fig. 2. Changes in soil $CaCl_2$-extractable phosphorus (a), citrate-extractable phosphorus (b), enzyme-extractable phosphorus (c), and HCl-extractable phosphorus (d) under different orchard–medicinal plant intercropping systems. Values represent means ± SEs. Different letters indicate significant differences at the $P < 0.05$ level. Pm: *Prunus salicina* monoculture; PH: *P. salicina* + *Hypericum monogynum*; PP: *P. salicina* + *Polygala fallax*; PR: *P. salicina* + *Rubus suavissmus*; PSI: *P. salicina* + *Semiliquidambar cathayensis* + *Illicium difengpi*.

$Shannon_{total}$), while richness/$Shannon_{rare}$ explained 95.7 % and 63.2 %.

3.4. Key regulatory factors influencing P fraction transformation

Complex correlations emerged between the soil biochemical properties and P fractions (Figs. 4 and 5). For instance, pH, C:P, and N:P ratios were significantly negatively correlated with citrate-P, HCl-P, enzyme-P, and AP, while TP exhibited positive correlations. ALP was negatively associated with MBP. RDA analysis indicated that the first two axes accounted for 64.1 % of the variance in P fractions (Fig. 5). Six significant environmental variables were identified: N:P ratio (32.0 %), moisture (24.1 %), ALP (13.5 %), TC (8.0 %), pH (7.4 %), and TP (6.2 %) (Fig. S3).

For all *phoD* communities, the Shannon index was negatively correlated with MBP but positively with HCl-P for the rare community (Table S4). C:P and N:P ratios were positively associated with richness and Shannon indices of the abundant community, but negatively with evenness; TP showed opposite trends. The all, abundant, and rare *phoD* communities were strongly linked to TP, C:P, and N:P ratios, while the rare community correlated with nearly all P fractions except $CaCl_2$-P (Fig. 4). Cyanobacteria, Planctomycetes, *Acidovorax*, *Actinomadura*, *Massilia*, and *Planctomyces* in all and abundant communities negatively correlated with citrate-P, HCl-P, enzyme-P, and AP, whereas Proteobacteria and *Bradyrhizobium* were positively correlated (Fig. S4). Few rare genera were associated with P fractions, though more rare than abundant genera correlated with MBP and ALP activity across OMIs, particularly in PH and PP systems (Tables S5 and S6).

Co-occurrence networks of various P fractions and *phoD*-harboring bacteria were constructed to investigate potential interactions (Fig. 6). The *phoD*-harboring bacteria associated with P fractions in OMIs varied significantly from those in Pm. Node and edge counts, positive correlations, average path length, and network degree in OMIs were lower than Pm, except for average path length and degree in PR (Table S7).

4. Discussion

4.1. Effects of OMIs on P pool distributions

OMIs altered the soil P fractions, with varying effects across medicinal plants (Figs. 1 and 2). In general, TP, AP, citrate-P, and HCl-P significantly decreased under OMIs, except in PR, compared with Pm systems. This is likely due to P depletion caused by intensified rhizosphere processes of intercropping plants (Wu et al., 2020), reflected in increased soil pH and high-P accumulation in leaf and root biomass (Tables S1 and S2). Additionally, OMIs, particularly in PH and PP, reduced enzyme-P but increased MBP, suggesting weaker P_o mineralization. Negative correlations between MBP and ALP as well as AP (Fig. 4) support this. OMIs enhance nutrient and water availability, improve soil structure via dense litter and roots, and promote microbial biosynthesis (Dai et al., 2020). This immobilizes labile P_i into MBP to sustain microbial metabolism (Liu et al., 2021a). As MBP is readily released, its short-term retention limits long-term P fixation in soil

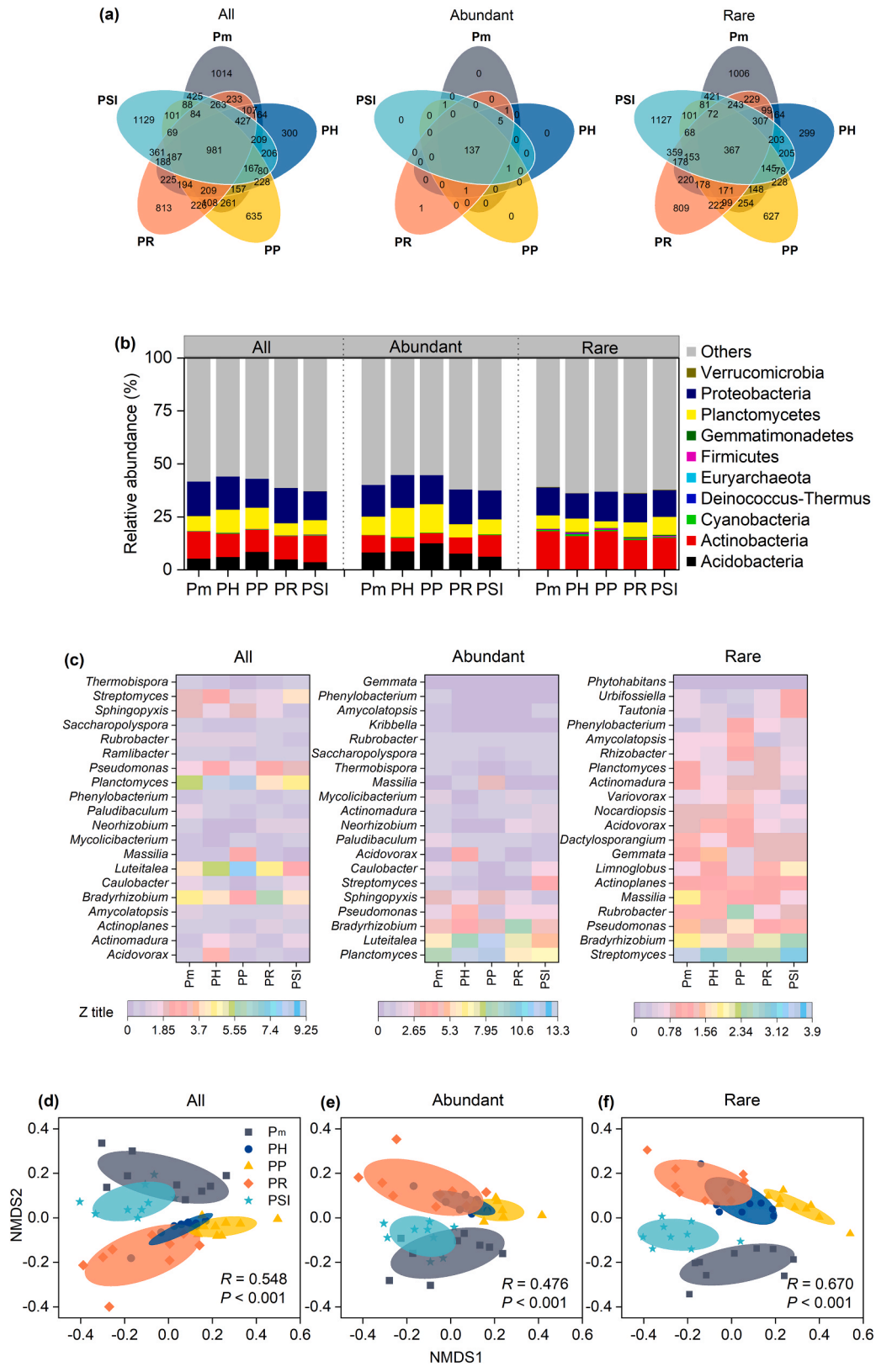

Fig. 3. Structure and composition of total, abundant, and rare *phoD*-harboring bacterial communities under different orchard–medicinal plant intercropping systems. Venn diagrams showing shared and unique *phoD*-harboring bacterial OTUs (a). Relative abundances of *phoD* communities at the phylum level (b) and for the top 20 genera (c). Nonmetric multidimensional scaling (NMDS) plots for *phoD* community structure based on the Bray–Curtis distance (d). Pm: *Prunus salicina* monoculture; PH: *P. salicina* + *Hypericum monogynum*; PP: *P. salicina* + *Polygala fallax*; PR: *P. salicina* + *Rubus suavissmus*; PSI: *P. salicina* + *Semiliquidambar cathayensis* + *Illicium difengpi*.

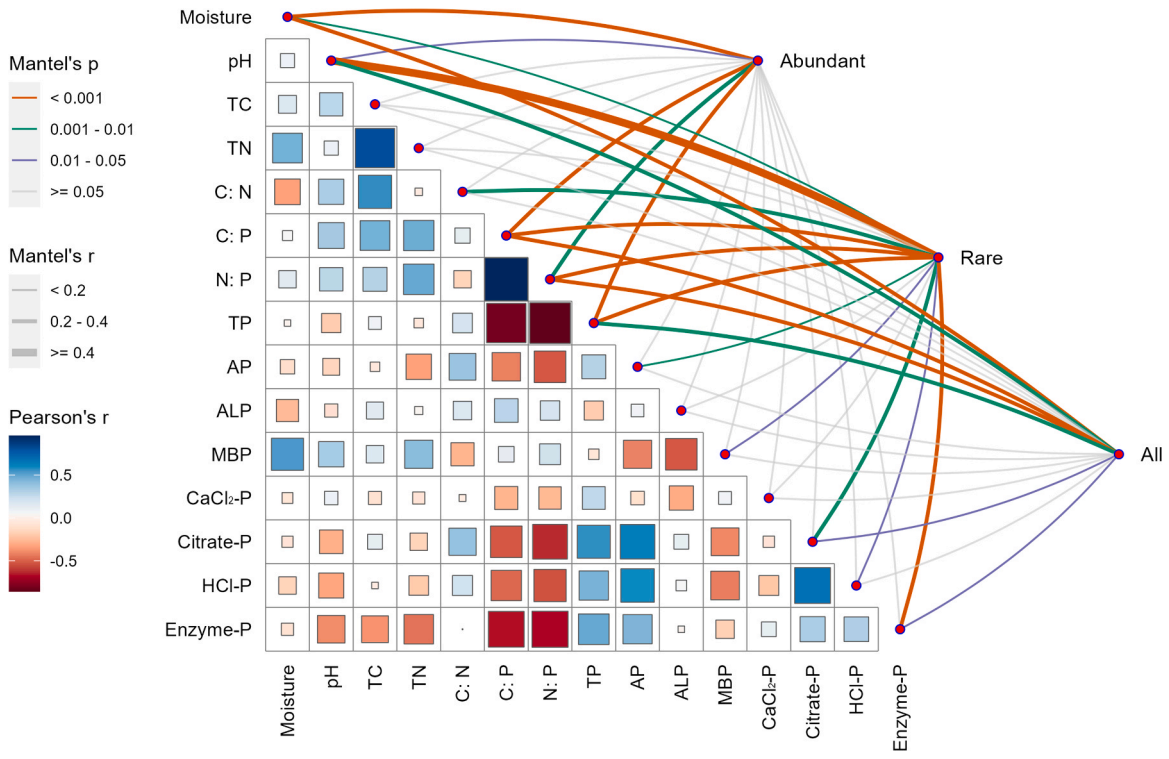

Fig. 4. Correlations among soil physiochemical traits, phosphorus (P) fractions, and *phoD*-harboring bacterial communities. Pairwise Spearman correlations among soil physiochemical properties and P fractions are represented by a color gradient. The Mantel test was used to assess the relationships between *phoD* community composition (total, abundant, and rare) and each soil trait or P fraction. Edge width corresponds to the Mantel r statistic, and edge color denotes statistical significance based on 999 permutations. TC: total carbon; TN: total nitrogen; TP: total phosphorus; AP: available phosphorus; ALP: alkaline phosphatase activity; MBP: microbial biomass phosphorus.

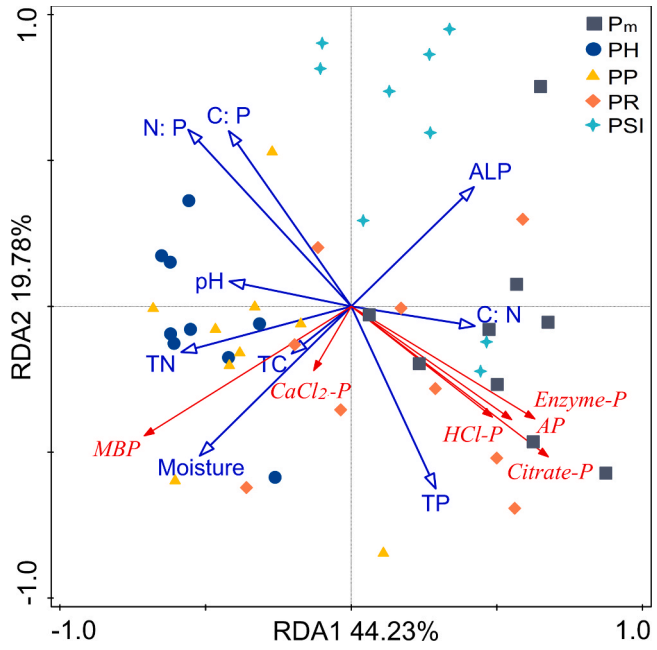

Fig. 5. Redundancy analysis (RDA) based on soil phosphorus fractions and physicochemical properties across different orchard–medicinal plant intercropping systems. TC: total carbon; TN: total nitrogen; TP: total phosphorus; ALP: alkaline phosphatase activity; AP: available phosphorus; MBP: microbial biomass phosphorus. Pm: *Prunus salicina* monoculture; PH: *P. salicina* + *Hypericum monogynum*; PP: *P. salicina* + *Polygala fallax*; PR: *P. salicina* + *Rubus suavissmus*; PSI: *P. salicina* + *Semiliquidambar cathayensis* + *Illicium difengpi*.

minerals (Katsalirou et al., 2016). This highlights MBP as a key labile P sink that supports intercropped plant growth (Dong et al., 2024). In contrast, $CaCl_2$-P remained unaffected by OMIs, as fine root biomass consistently intercepted solution P_i (Wu et al., 2019), and P mobilization was constrained by N cation saturation (Wei et al., 2019). This stability indicates that OMIs do not markedly increase the risk of surface P runoff in the karst region (< 13.9 mg kg^{-1} P environmental threshold) (Zhu et al., 2022). However, as observed in PR, intercropping, mixed plantations, or cover crops can variably impact biologically available P depending on litter quality and quantity mediating chemical-microbial processes (Dong et al., 2024; Kim Hoang and Marschner, 2017; Wan et al., 2022; Wang et al., 2023b).

The relative ratios of soil P fractions indicate P activation, supply capacity, and acquisition strategies, serving as key soil fertility indicators, which depend on the chemical form and size of the P pool (Crain et al., 2018; Zhu et al., 2022). The AP/TP ratio (i.e., P activation capacity [PAC]) is used for assessing P bioavailability and improvement potential (Liu et al., 2025). Higher PAC values (>2.0 %) indicate easier conversion of soil TP to AP (Wu et al., 2017). PACs in OMIs, particularly PH and PP, were lower than Pm (Table S3), reflecting weak P activation. Conversely, the MBP/TP ratio, microbial metabolic quotient for P, was higher in OMIs, highlighting microbial strategies to recycle and retain nutrients through biomass under nutrient-poor conditions (Chen et al., 2021; Gao et al., 2024). Effective ratios from the BBP method quantify biological mechanisms (Crain et al., 2018). P fractions in OMIs followed HCl-P > citrate-P > $CaCl_2$-P > enzyme-P, indicating that bioavailable P is primarily inorganic, aligning with prior studies (Wang et al., 2023a, 2023b). Ratios of HCl-P/$CaCl_2$-P and citrate-P/$CaCl_2$-P exceeding 1 in OMIs suggest acid and proton release enhance P acquisition for medicinal plants beyond $CaCl_2$-P uptake in soil pore water (Qi et al., 2022). Ratios of citrate-P/enzyme-P and HCl-P/enzyme-P above 1 in OMIs indicate acids surpass phosphatase and phytase in P acquisition,

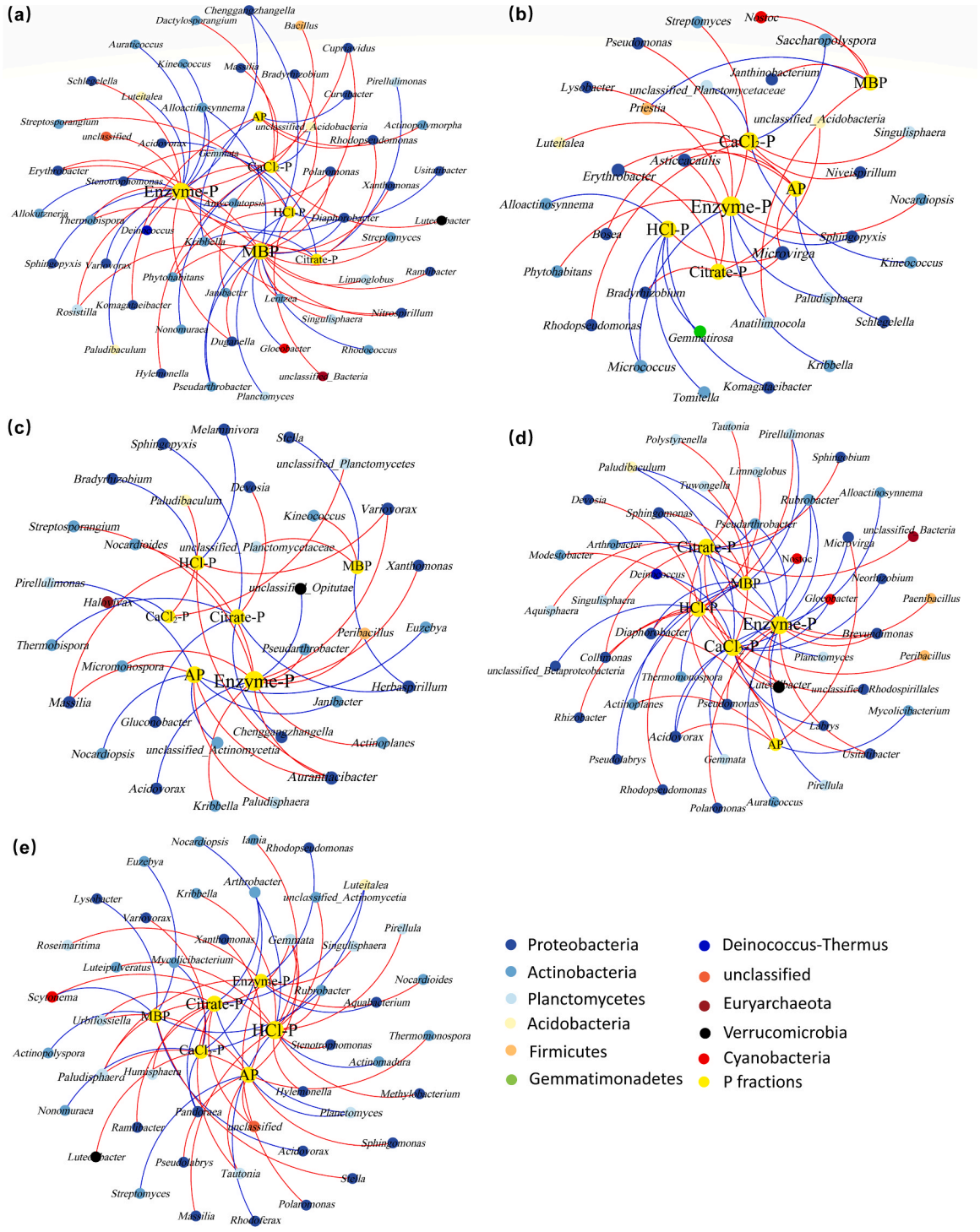

Fig. 6. Co-occurrence network analysis of *phoD*-harboring bacterial communities and phosphorus fractions under different orchard–medicinal plant intercropping systems. (a) *Prunus salicina* monoculture (Pm), (b) *P. salicina* + *Hypericum monogynum* (PH), (c) *P. salicina* + *Polygala fallax* (PP), (d) *P. salicina* + *Rubus suavissmus* (PR), and (e) *P. salicina* + *Semiliquidambar cathayensis* + *Illicium difengpi* (PSI). Red solid lines indicate significant positive correlations ($r > 0.50$, $P < 0.05$), whereas blue lines denote significant negative correlations ($r < -0.50$, $P < 0.05$). $CaCl_2$-P: $CaCl_2$-extractable phosphorus; Citrate-P: citrate-extractable phosphorus; Enzyme-P: enzyme-extractable phosphorus; HCl-P: HCl-extractable phosphorus; AP: available phosphorus; MBP: microbial biomass phosphorus.

contrasting the finding in mesic vegetation in northern Wales (DeLuca et al., 2015). However, OMIs reduced the acid dissolution of P_i, negatively affecting P availability. Overall, OMIs, except PR, shifted biological P-use strategies from P_i acquisition to temporary P_o preservation, increasing P-use efficiency depending on the specific medicinal plant.

4.2. *Effects of OMIs on phoD-harboring bacterial community and ALP activity*

The composition and structure of abundant and rare *phoD*-harboring bacteria varied significantly with OMIs (Fig. 3). Shared OTUs decreased in OMIs compared with Pm systems (Fig. 3a), likely due to an increase in macroaggregates with smaller specific surface areas, larger pores, and

lower clay content (Liu et al., 2023a; Zeng et al., 2024), conditions unfavorable for microbial survival (Yang et al., 2023). The dominant *phoD*-harboring phyla, including Proteobacteria, Actinobacteria, and Planctomycetes, remained consistent across all systems (Fig. 3b). This reflects stability in P_o-hydrolyzing microbial guilds across agroforestry systems and environments (Hu et al., 2018; Lagos et al., 2016). However, Firmicutes, Gemmatimonadetes, Verrucomicrobia, Deinococcus-Thermus, and Euryarchaeota were unique among the rare taxa within OMIs. Actinobacteria (K-strategists) replaced Acidobacteria (r-strategists) as the dominant taxon, driven by critical genera such as *Streptomyces* and *Rubrobacter*, whose relative abundances varied with OMIs (Fig. 3c), indicating microbial synergy. Rare taxa showed weak correlations with soil nutrients (Fig. S4), suggesting limited capacity for resource use or competition under OMIs-induced environmental changes compared with abundant taxa (Wan et al., 2021; Wei et al., 2019). NMDS analysis revealed distinct *phoD* community structures by OMIs, with rare communities showing up to 67 % variability (Fig. 3d), likely influenced by intercropped medicinal plants with differing root systems (e.g., extensive horizontal roots in PR) affecting soil stoichiometry and plant properties (Tables S1 and S2). OMIs minimally impacted the *phoD* diversity (Fig. S1), likely due to stable soil pH, a key driver of bacterial diversity (Liu et al., 2019; Ragot et al., 2016). These findings indicate distinct responses of abundant and rare *phoD* communities to OMIs, with rare taxa being more sensitive.

The *phoD* gene encodes the soil ALP protein, playing a key role in regulating P bioavailability (Bergkemper et al., 2016; Cao et al., 2022). A strong positive correlation was found between rare *phoD*-harboring genera (e.g., *Neorhizobium* and *Humisphaera*) and ALP activity, while abundant genera (e.g., *Massilia* and *Usitatibacter*) showed negative correlations (Table S5). Furthermore, the rare community structure and higher rare taxon presence were significantly linked to increased ALP activity in OMIs compared with Pm systems, particularly PH and PP (Fig. 4 and Table S6). These findings support previous studies highlighting a stronger association between ALP activity and rare, rather than abundant, *phoD* bacterial taxa across ecosystems (Liu et al., 2021b; Wei et al., 2019; Xiong and Wan, 2023). This suggests that rare *phoD*-harboring communities disproportionately influence P availability via ALP activity after OMIs establishment, driven by microbial activity changes and organic substrate inputs. However, neither abundant nor rare *phoD* community diversity correlated significantly with ALP activity (Table S4), consistent with findings across varied climates and land uses (Ragot et al., 2017). This discrepancy likely stems from universal primers capturing only a subset of *phoD* genes capable of producing ALP (Hu et al., 2018; Li et al., 2021). These processes depend on environmental factors operating across temporal and spatial scales (Xu et al., 2022). Additionally, potential ALP activity reflects stable enzymes persisting in soil, rather than just current microbial ALP production (Burns et al., 2013; Ragot et al., 2017).

4.3. Driving factors influencing soil P bioavailability

The effects of intercropping medicinal plants on soil physicochemical properties and P bioavailability varied by the form of bioavailable P (Wang et al., 2023b; Zhang et al., 2020). In this study, HCl-P, citrate-P, and enzyme-P were negatively influenced by pH, N:P, and C:P but positively correlated with AP and TP (Figs. 4 and 5), suggesting that these fractions are major contributors to AP. Previous studies have identified pH and C:N:P stoichiometry as key regulators of microbial P-solubilization and mineralization, shaping P cycling (Dai et al., 2020; Wan et al., 2021; Yin et al., 2023). RDA analysis highlighted N:P, moisture, pH, and ALP as significant factors affecting bioavailable P in OMIs within karst soils (Fig. S3), emphasizing the substantial impact of water scarcity on P availability in this region. Thus, OMIs were found to increase soil moisture (Table S1), promoting the conversion of bioavailable P (Hu et al., 2018). This aligns with reports that agroforestry systems alter *phoD*-harboring bacterial communities by modifying environmental conditions (Ragot et al., 2017; Xie et al., 2020). Higher soil moisture positively influenced MBP, while ALP negatively correlated with MBP, suggesting that ALP degrades unstable MBP (Dai et al., 2020; Dong et al., 2024). ALP-producing microorganisms likely target unstable MBP during metabolism. Additionally, MBP was negatively associated with HCl-P and citrate-P, indicating that intercropped plants reduce AP by fixing excess P through MBP, maintaining bioavailable P balance for plant absorption. The root TP content and biomass negatively correlated with HCl-P and citrate-P, suggesting that the intercropped roots absorb more P via organic acid secretion or proton regulation, reducing P bioavailability and AP. Higher plant P uptake under intercropping systems increases plant contribution to P cycling. MBP is critical in soil P dynamics, replenishing P in the soil solution during deficiency and facilitating plant absorption (Gao et al., 2024). TP in leaves and roots showed a positive correlation with MBP, indicating that increased MBP enhances plant P status, promoting growth and nutrient uptake. These findings demonstrate that higher soil MBP improves plant P absorption and utilization efficiency.

Microorganisms contribute to biomass formation and enhance their activity, increasing the P activation rate and bioavailable P content through P retention. The *phoD*-harboring bacterial community is vital for P_o mineralization and P_i dissolution (Tian et al., 2022; Wei et al., 2021). A strong correlation was observed between rare community structure and bioavailable P fractions, excluding $CaCl_2$-P, while abundant community structure showed no such correlation (Figs. 4 and S4). This relationship is indirectly influenced by the pH and C:N:P stoichiometry. Abundant *Bradyrhizobium* positively affected HCl-P, citrate-P, and enzyme-P, while rare *Pseudomonas* positively influenced citrate-P (Fig. S4). *Bradyrhizobium* (Dong et al., 2024) and *Pseudomonas* (Zhang et al., 2023) enhance plant-available P, particularly under organic amendments serving as the primary carbon source (Hu et al., 2018). Their elevated abundance under OMIs, compared with Pm, likely contributes to increased soil P_i solubilization and depletion, as these taxa show significant correlations with HCl-P, citrate-P, and enzyme-P (Fig. S4), thereby promoting biologically driven P availability in the intercropped rhizospheres (Wang et al., 2023a). However, nutrient competition with host plants (Zhang et al., 2023), led rare genera such as *Actinoplanes* and *Amycolatopsis*, along with abundant taxa including *Acidovorax*, *Massilia*, and *Planctomyces*, to negatively affect HCl-P, citrate-P, and enzyme-P, consequently increasing MBP concentrations in OMIs (Fig. 1). Network analysis revealed fewer interactions among *phoD*-harboring bacteria under PH and PP compared with Pm (Table S7), implying reduced bacterial synergy and assembly (Yin et al., 2023), likely due to insufficient AP under PH and PP (Fig. 1). The *phoD*-harboring bacteria associated with various P fractions under OMIs diverged markedly from those observed in Pm systems (Fig. 6), likely due to differences in P fraction production and utilization (Wang et al., 2024). These findings suggest that OMIs altered the relationships between *phoD*-harboring bacteria (particularly rare taxa) and P fractions, helping explain P fraction changes in OMIs. These microbial shifts may cascade into nitrogen transformation (via enzymatic competition) and potassium availability (through cation exchange), necessitating systematic future study. However, despite these shifts, overall microbial diversity under OMIs did not influence biological P cycling (Table S4), which contrasts with the findings of Chen et al. (2023). Overall, the findings suggest that P bioavailability is more sensitive to community structure than diversity.

$CaCl_2$-P, a soluble and weakly adsorbed P_i, remained largely unaffected by intercropping plants, soil physicochemical properties, and the *phoD*-harboring bacterial community, except for its positive regulation by TP (Fig. 4, Tables S4 and S5). Similarly, Wang et al. (2023b) observed a positive correlation between $CaCl_2$-P and MBP. However, other studies report that $CaCl_2$-P is influenced by factors like tree species richness, soil organic matter, moisture, pH, and bacterial diversity (Wu et al., 2019; Zhu et al., 2022). Certain rare taxa, including *Verrucomicrobia*, *Actinomadura*, *Aurantimonas*, *Luteitalea*, *Luteolibacter*, and *Tuwongella*, were

significantly correlated with $CaCl_2$-P (Fig. S4), suggesting their role in increasing bioavailable P and enhancing rhizosphere P acquisition in karst areas (Wang et al., 2023a). Microbial alteration of the P reservoirs in low-P soils rarely affects $CaCl_2$-P but undergoes significant changes in high-P environments (Li et al., 2024). The specific transformation mechanisms of $CaCl_2$-P in karst calcareous soils warrant further investigation.

4.4. Implications of karst soil P nutrient management in OMIs

OMIs are designed to enhance soil health and ecosystem functionality, thereby boosting smallholder income (Pérez-Nicolás et al., 2018). Nonetheless, interspecific competition for limited resources can emerge under OMIs (Zhang et al., 2020), especially in fragile, nutrient-poor karst landscapes where water and nutrient scarcity are common. P deficiency and limited biological P availability are pervasive issues in karst soils (Dong et al., 2024; Li et al., 2025), and these issues are further exacerbated by rocky desertification associated with long-term orchard monoculture. Interplanting medicinal plants in such orchards resulted in differential impacts on soil P reservoir (Figs. 1 and 2). PH and PP systems improved P-use efficiency, whereas PR contributed more to maintaining overall P pool stability, and PSI exhibits an intermediate level relative to both conditions. Our previous studies have shown that PH and PP improve soil structure (Zeng et al., 2024), while PR and PSI enhance water-use efficiency (Tao et al., 2024). These findings highlight the complexity of OMIs and the necessity for region-specific intercropping strategies (Liu et al., 2021a). For karst orchards, selection of intercropped medicinal species should align with their ecological contributions, not merely economic returns. To support efficient P cycling, deep-rooted and foliage-rich species are recommended, as roots and litter represent critical P sources in karst systems (Liu et al., 2023b), with their effects intensifying over time (Wu et al., 2020). In this context, PR and subsequent PSI system appears optimal due to its dual economic (medicinal leaves with the highest market price) and ecological advantages. Phosphate fertilizer application should also aim to optimize *phoD*-harboring bacterial communities during key intercropping stages (Hu et al., 2018), ultimately boosting plant productivity, sustainability, and ecological resilience. As this study is limited to short-term observations with one-time base fertilization, long-term field experiments involving varied medicinal species and continuous fertilization (timing and type) are required under changing environmental conditions.

5. Conclusions

This study demonstrated the divergent effects of intercropping different medicinal plants on soil P bioavailability and the *phoD*-harboring bacterial community in karst regions. OMIs reduced bioavailable P fractions except for $CaCl_2$-P, while increasing MBP, particularly in PH and PP systems, suggesting enhanced plant P uptake at the expense of rhizosphere AP. Rare *phoD*-harboring bacteria exhibited greater sensitivity to OMIs than abundant taxa and played a dominant role in regulating bioavailable P, which was influenced by soil N:P, pH, moisture, and ALP activity. Key genera, such as abundant *Bradyrhizobium* and rare *Pseudomonas*, were critical drivers of soil P availability. With the exception of PR, OMIs shifted P utilization strategies from P_i acquisition to P_o temporary storage, thereby improving P-use efficiency via rare *phoD* community modulation. These findings advance our understanding of microbial-mediated P cycling in karst agroecosystems. Future research should explore long-term dynamics of rhizosphere P cycling, incorporating root functional traits and optimizing P fertilization regimes for sustainable OMIs management.

CRediT authorship contribution statement

Chuan Jiang: Supervision, Methodology, Formal analysis. **Xiaoling Zeng:** Methodology, Investigation, Data curation. **Yuanyang Chen:** Investigation, Formal analysis, Data curation. **Yanqiang Jin:** Writing – review & editing, Supervision, Methodology, Formal analysis. **Akash Tariq:** Software, Formal analysis. **Shujie Chen:** Investigation, Formal analysis. **Belayneh Azene:** Writing – review & editing, Conceptualization. **Fuzhao Huang:** Writing – review & editing, Supervision, Funding acquisition, Conceptualization. **Chenggang Liu:** Writing – original draft, Project administration, Methodology, Investigation, Formal analysis, Data curation, Conceptualization.

Funding

This work was supported by the Guangxi Natural Science Foundation Program of China (2022GXNSFDA035076), the National Natural Science Foundation of China (32271854, 32260286), the Fund of Guangxi Key Laboratory of Plant Conservation and Restoration Ecology in Karst Terrain (22−035−26), the 'Yunnan Revitalization Talent Support Program' in Yunnan Province (XDYC-QNRC-2022–0204), and the 'Light of West China Program' of CAS.

Declaration of Competing Interest

The authors declare that they have no known competing financial interests or personal relationships that could have appeared to influence the work reported in this paper.

Acknowledgements

We thank the Institutional Center for Shared Technologies and Facilities of Xishuangbanna Tropical Botanical Garden, Chinese Academy of Sciences (CAS), for laboratory analysis.

Appendix A. Supporting information

Supplementary data associated with this article can be found in the online version at doi:10.1016/j.agee.2025.109881.

Data availability

Data will be made available on request.

References

Applequist, W.L., Brinckmann, J.A., Cunningham, A.B., Hart, R.E., Heinrich, M., Katerere, D.R., van Andel, T., 2020. Scientists' warning on climate change and medicinal plants. Planta Med. 86, 10–18. https://doi.org/10.1055/a-1041-3406.

Bergkemper, F., Schöler, A., Engel, M., Lang, F., Krüger, J., Schloter, M., Schulz, S., 2016. Phosphorus depletion in forest soils shapes bacterial communities towards phosphorus recycling systems. Environ. Microbiol. 18, 1988–2000. https://doi.org/10.1111/1462-2920.13188.

Burns, R.G., DeForest, J.L., Marxsen, J., Sinsabaugh, R.L., Stromberger, M.E., Wallenstein, M.D., Weintraub, M.N., Zoppini, A., 2013. Soil enzymes in a changing environment: current knowledge and future directions. Soil Biol. Biochem. 58, 216–234. https://doi.org/10.1016/j.soilbio.2012.11.009.

Cao, N., Zhi, M., Zhao, W., Pang, J., Hu, W., Zhou, Z., Meng, Y., 2022. Straw retention combined with phosphorus fertilizer promotes soil phosphorus availability by enhancing soil P-related enzymes and the abundance of *phoC* and *phoD* genes. Soil Till. Res. 220, 105390. https://doi.org/10.1016/j.still.2022.105390.

Chen, S.L., Yu, H., Luo, H.M., Wu, Q., Li, C.F., Steinmetz, A., 2016. Conservation and sustainable use of medicinal plants: problems, progress, and prospects. Chin. Med. 11, 37. https://doi.org/10.1186/s13020-016-0108-7.

Chen, X., Condron, L.M., Dunfield, K.E., Wakelin, S.A., Chen, L., 2021. Impact of grassland afforestation with contrasting tree species on soil phosphorus fractions and alkaline phosphatase gene communities. Soil Biol. Biochem. 159, 108274. https://doi.org/10.1016/j.soilbio.2021.108274.

Chen, X., Wang, Y., Wang, J., Condron, L.M., Guo, B., Liu, J., Qiu, G., Li, H., 2023. Impact of ryegrass cover crop inclusion on soil phosphorus and *pqqC*- and *phoD*-harboring bacterial communities. Soil Till. Res. 234, 105823. https://doi.org/10.1016/j.still.2023.105823.

Cheng, H., Hu, W., Zhou, X., Dong, R., Liu, G., Li, Q., Zhang, X., 2022. Fruit tree legume herb intercropping orchard system is an effective method to promote the sustainability of systems in a karst rocky desertification control area. Forests 13, 1536. https://doi.org/10.3390/f13101536.

Crain, G.M., McLaren, J.R., Brunner, B., Darrouzet-Nardi, A., 2018. Biologically available phosphorus in biocrust-dominated soils of the Chihuahuan desert. Soil Syst. 2, 56. https://doi.org/10.3390/soilsystems2040056.

Dai, Z., Liu, G., Chen, H., Chen, C., Wang, J., Ai, S., Wei, D., Li, D., Ma, B., Tang, C., Brookes, P.C., Xu, J., 2020. Long-term nutrient inputs shift soil microbial functional profiles of phosphorus cycling in diverse agroecosystems. ISME J. 14, 757–770. https://doi.org/10.1038/s41396-019-0567-9.

DeLuca, T.H., Glanville, H.C., Harris, M., Emmett, B.A., Pingree, M.R., de Sosa, L.L., Cerdá-Moreno, C., Jones, D.L., 2015. A novel biologically-based approach to evaluating soil phosphorus availability across complex landscapes. Soil Biol. Biochem. 88, 110–119. https://doi.org/10.1016/j.soilbio.2015.05.016.

Deng, J., Fang, S., Fang, X., Jin, Y., Kuang, Y., Lin, F., Liu, J., Ma, J., Nie, Y., Ouyang, S., Ren, J., Tie, L., Tang, S., Tan, X., Wang, X., Fan, Z., Wang, Q., Wang, H., Liu, C., 2023. Forest understory vegetation study: current status and future trends. For. Res. 3, 6. https://doi.org/10.48130/FR-2023-0006.

Dong, R., Hu, W., Bu, L., Cheng, H., Liu, G., 2024. Legume cover crops alter soil phosphorus availability and microbial community composition in mango orchards in karst areas. Agr. Ecosyst. Environ. 364, 108906. https://doi.org/10.1016/j.agee.2024.108906.

Fraser, T.D., Lynch, D.H., Bent, E., Entz, M.H., Dunfield, K.E., 2015. Soil bacterial *phoD* gene abundance and expression in response to applied phosphorus and long-term management. Soil Biol. Biochem. 88, 137–147. https://doi.org/10.1016/j.soilbio.2015.04.014.

Gao, D., Shi, W., Wang, H., Liu, Z., Jiang, Q., Lv, W., Wang, S., Zhang, Y.L., Zhao, C., Hagedorn, F., 2024. Contrasting global patterns of soil microbial quotients of carbon, nitrogen, and phosphorus in terrestrial ecosystems. Catena 243, 108145. https://doi.org/10.1016/j.catena.2024.108145.

Guo, Y., Li, Y., Li, J., Li, J., Wen, S., Huang, F., He, W., Wang, B., Lu, S., Li, D., Xiang, W., Li, X., 2022. Comparison of aboveground vegetation and soil seed bank composition among three typical vegetation types in the karst regions of Southwest China. Agronomy 12, 1871. https://doi.org/10.3390/agronomy12081871.

Hu, Y., Xia, Y., Sun, Q., Liu, K., Chen, X., Ge, T., Zhu, B., Zhu, Z., Zhang, Z., Su, Y., 2018. Effects of long-term fertilization on *phoD*-harboring bacterial community in Karst soils. Sci. Total Environ. 628–629, 53–63. https://doi.org/10.1016/j.scitotenv.2018.01.314.

Katsalirou, E., Deng, S., Gerakis, A., Nofziger, D.L., 2016. Long-term management effects on soil P, microbial biomass P, and phosphatase activities in prairie soils. Eur. J. Soil Biol. 76, 61–69. https://doi.org/10.1016/j.ejsobi.2016.07.001.

Kim Hoang, K.T., Marschner, P., 2017. Plant and microbial-induced changes in P pools in soil amended with straw and inorganic P. J. Soil Sci. Plant Nutr. 17, 1088–1101. https://doi.org/10.4067/s0718-95162017000400018.

Lagos, L.M., Acuña, J.J., Maruyama, F., Ogram, A., de la Luz Mora, M., Jorquera, M.A., 2016. Effect of phosphorus addition on total and alkaline phosphomonoesterase-harboring bacterial populations in ryegrass rhizosphere microsites. Biol. Fert. Soils 52, 1007–1019. https://doi.org/10.1007/s00374-016-1137-1.

Li, J., Xie, T., Zhu, H., Zhou, J., Li, C., Xiong, W., Xu, L., Wu, Y., He, Z., Li, X., 2021. Alkaline phosphatase activity mediates soil organic phosphorus mineralization in a subalpine forest ecosystem. Geoderma 404, 115376. https://doi.org/10.1016/j.geoderma.2021.115376.

Li, J., Wang, H., You, Y., Wang, J., Tong, X., Hu, J., Ming, A., Chen, L., Liu, S., 2024. Effects of tree species assembly on bioavailable P components in rhizosphere soil of southern subtropical plantation. Chin. J. Appl. Ecol. 35, 1492–1500. https://doi.org/10.13287/j.1001-9332.202406.018.

Li, Z., Qin, W., You, Y., Chen, J., Zhao, X., Dong, R., Gu, X., Cui, S., Chen, C., Stirling, E., Xue, R., 2025. Land use patterns change N and P cycling bacterial diversity in an acidic karst soil. Agr. Ecosyst. Environ. 380, 109389. https://doi.org/10.1016/j.agee.2024.109389.

Liu, C., Jin, Y., Liu, C., Tang, J., Wang, Q., Xu, M., 2018. Phosphorous fractions in soils of rubber-based agroforestry systems: influence of season, management and stand age. Sci. Total Environ. 616–617, 1576–1588. https://doi.org/10.1016/j.scitotenv.2017.10.156.

Liu, C., Jin, Y., Hu, Y., Tang, J., Xiong, Q., Xu, M., Bibi, F., Beng, K.C., 2019. Drivers of soil bacterial community structure and diversity in tropical agroforestry systems. Agr. Ecosyst. Environ. 278, 24–34. https://doi.org/10.1016/j.agee.2019.03.015.

Liu, C., Wang, Q., Jin, Y., Tang, J., Lin, F., Olatunji, O.A., 2021a. Perennial cover crop biomass contributes to regulating soil P availability more than rhizosphere P-mobilizing capacity in rubber-based agroforestry systems. Geoderma 401, 115218. https://doi.org/10.1016/j.geoderma.2021.115218.

Liu, C., Jin, Y., Lin, F., Jiang, C., Zeng, X., Feng, D., Huang, F., Tang, J., 2023a. Land use change alters carbon and nitrogen dynamics mediated by fungal functional guilds within soil aggregates. Sci. Total Environ. 902, 166080. https://doi.org/10.1016/j.scitotenv.2023.166080.

Liu, J., Liang, Y., Xiao, F., Han, Y., Hu, C., Wei, L., Duan, M., 2023b. Main sources of soil phosphorus and their seasonal changes across different vegetation restoration stages in Karst region of southwest China. Chin. J. Appl. Ecol. 34, 3313–3321. https://doi.org/10.13287/j.1001-9332.202312.016.

Liu, Q., Zhou, W., Yang, Z., Wang, T., Fu, Y., Yue, X., X, H., Tao, Y., Deng, F., Lei, X., Chen, Y., Ren, W., 2025. Potato–rice and garlic–rice rotation increases soil phosphorus availability through phosphate-solubiliing bacteria and root exudates in upland–paddy cropping systems. Agr. Ecosyst. Environ. 390, 109721. https://doi.org/10.1016/j.agee.2025.109721.

Liu, S., Zhang, X., Dungait, J.A.J., Quine, T.A., Razavi, B.S., 2021b. Rare microbial taxa rather than *phoD* gene abundance determine hotspots of alkaline phosphomonoesterase activity in the karst rhizosphere soil. Biol. Fert. Soils 57, 257–268. https://doi.org/10.1007/s00374-020-01522-4.

Lu, S., Sun, H., Zhou, Y., Qin, F., Guan, X., 2020. Examining the impact of forestry policy on poor and non-poor farmers' income and production input in collective forest areas in China. J. Clean. Prod. 276, 123784. https://doi.org/10.1016/j.jclepro.2020.123784.

Malik, M.A., Marschner, P., Khan, K.S., 2012. Addition of organic and inorganic P sources to soil–Effects on P pools and microorganisms. Soil Biol. Biochem 49, 106–113. https://doi.org/10.1016/j.soilbio.2012.02.013.

Pérez-Nicolás, M., Vibrans, H., Romero-Manzanares, A., 2018. Can the use of medicinal plants motivate forest conservation in the humid mountains of Northern Oaxaca, Mexico? Bot. Sci. 96, 267–285. https://doi.org/10.17129/botsci.1862.

Qi, X., Chen, L., Zhu, J.-a, Li, Z., Lei, H., Shen, Q., Wu, H., Ouyang, S., Zeng, Y., Hu, Y., Xiang, W., 2022. Increase of soil phosphorus bioavailability with ectomycorrhizal tree dominance in subtropical secondary forests. For. Ecol. Manag. 521, 120435. https://doi.org/10.1016/j.foreco.2022.120435.

Ragot, S.A., Huguenin-Elie, O., Kertesz, M.A., Frossard, E., Bünemann, E.K., 2016. Total and active microbial communities and *phoD* as affected by phosphate depletion and pH in soil. Plant Soil 408, 15–30. https://doi.org/10.1007/s11104-016-2902-5.

Ragot, S.A., Kertesz, M.A., Mészáros, É., Frossard, E., Bünemann, E.K., 2017. Soil *phoD* and *phoX* alkaline phosphatase gene diversity responds to multiple environmental factors. FEMS Microbiol. Ecol. 93, fiw212. https://doi.org/10.1093/femsec/fiw212.

Roy, J., Biswas, D.R., Basak, B.B., Bhattacharyya, R., Das, S., Biswas, S., Dass, A., Rupesh, T., Singh, Ak, Ghosh, A., 2025. Long-term impact of silviculture systems on phosphorus transformation and adsorption behaviour in semi-arid restored lands. Agr. Ecosyst. Environ. 381, 109449. https://doi.org/10.1016/j.agee.2024.109449.

Spohn, M., Kuzyakov, Y., 2013. Distribution of microbial-and root-derived phosphatase activities in the rhizosphere depending on P availability and C allocation–Coupling soil zymography with ^{14}C imaging. Soil Biol. Biochem. 67, 106–113. https://doi.org/10.1016/j.soilbio.2013.08.015.

Tao, W., Huang, F., Li, J., Wang, Z., Luo, T., Lu, F., Li, X., 2024. Plant water use efficiency of different intercropping patterns in the karst area of the Lijiang river watershed. For. Grassl. Resour. Res. 2, 34–42. https://doi.org/10.13466/j.cnki.lczyyj.2024.02.005.

Tian, J., Lu, X., Chen, Q., Kuang, X., Liang, C., Deng, L., Lin, D., Cai, K., Tian, J., 2022. Phosphorus fertilization affects soybean rhizosphere phosphorus dynamics and the bacterial community in karst soils. Plant Soil 475, 137–152. https://doi.org/10.1007/s11104-020-04662-6.

Wan, S., Lin, G., Liu, B., Ding, Y., Li, S., Mao, R., 2022. Contrasting responses of soil phosphorus pool and bioavailability to alder expansion in a boreal peatland, Northeast China. Catena 212, 106128. https://doi.org/10.1016/j.catena.2022.106128.

Wan, W., He, D., Li, X., Xing, Y., Liu, S., Ye, L., Yang, Y., 2021. Linking rare and abundant phoD-harboring bacteria with ecosystem multifunctionality in subtropical forests: from community diversity to environmental adaptation. Sci. Total Environ. 796, 148943. https://doi.org/10.1016/j.scitotenv.2021.148943.

Wang, H., Tian, D., Liu, H., Wang, Z., He, Y., Lu, J., Zhu, Y., Wei, S., Wang, H., Wu, L., Chen, L., 2024. Rare rather than abundant taxa of soil bacteria and fungi regulate soil multifunctionality in Eucalyptus plantations. Catena 245, 108303. https://doi.org/10.1016/j.catena.2024.108303.

Wang, M., Huang, L., Liang, H., Wen, X., Liu, H., Ren, H., Tang, H., 2021. Conservation introduction of *Illicium difengpi*, an endangered medicinal plant in southern China is feasible. Glob. Ecol. Conserv 30, e01756. https://doi.org/10.1016/j.gecco.2021.e01756.

Wang, M., Wu, Y., Zhao, J., Liu, Y., Chen, Z., Tang, Z., Tian, W., Xi, Y., Zhang, J., 2022. Long-term fertilization lowers the alkaline phosphatase activity by impacting the *phoD*-harboring bacterial community in rice-winter wheat rotation system. Sci. Total Environ. 821, 153406. https://doi.org/10.1016/j.scitotenv.2022.153406.

Wang, W., Yin, F., Gu, J., Wang, Z., Zhang, F., Li, L., Cheng, Z., 2023b. Effects of maize/soybean intercropping on rhizosphere soil phosphorus availability and functional genes involved in phosphorus cycling in Northwest China. Plant Soil 506, 407–420. https://doi.org/10.1007/s11104-023-06363-2.

Wang, W., Chen, Y., Zhang, F., Zhang, W., Liu, J., Wang, J., Yin, F., Cheng, Z., 2023a. Cotton-maize intercropping increases rhizosphere soil phosphorus bioavailability by regulating key phosphorus cycling genes in northwest China. Appl. Soil Ecol. 182, 104734. https://doi.org/10.1016/j.apsoil.2022.104734.

Wei, X., Hu, Y., Razavi, B.S., Zhou, J., Shen, J., Nannipieri, P., Wu, J., Ge, T., 2019. Rare taxa of alkaline phosphomonoesterase-harboring microorganisms mediate soil phosphorus mineralization. Soil Biol. Biochem. 131, 62–70. https://doi.org/10.1016/j.soilbio.2018.12.025.

Wei, X., Hu, Y., Cai, G., Yao, H., Ye, J., Sun, Q., Veresoglou, S.D., Li, Y., Zhu, Z., Guggenberger, G., Chen, X., Su, Y., Li, Y., Wu, J., Ge, T., 2021. Organic phosphorus availability shapes the diversity of *phoD*-harboring bacteria in agricultural soil. Soil Biol. Biochem. 161, 108364. https://doi.org/10.1016/j.soilbio.2021.108364.

Wu, H., Xiang, W., Ouyang, S., Forrester, D.I., Zhou, B., Chen, L., Ge, T., Lei, P., Chen, L., Zeng, Y., Song, X., Peñuelas, J., Peng, C., Gallery, R., 2019. Linkage between tree species richness and soil microbial diversity improves phosphorus bioavailability. Funct. Ecol. 33, 1549–1560. https://doi.org/10.1111/1365-2435.13355.

Wu, H., Xiang, W., Chen, L., Ouyang, S., Xiao, W., Li, S., Forrester, D.I., Lei, P., Zeng, Y., Deng, X., Zeng, L., Kuzyakov, Y., 2020. Soil phosphorus bioavailability and recycling increased with stand age in Chinese Fir plantations. Ecosystems 23, 973–988. https://doi.org/10.1007/s10021-019-00450-1.

Wu, Q., Zhang, S., Zhu, P., Huang, S., Wang, B., Zhao, L., Xu, M., 2017. Characterizing differences in the phosphorus activation coefficient of three typical cropland soils and the influencing factors under long-term fertilization. PLoS One 12, e0176437. https://doi.org/10.1371/journal.pone.0176437.

Xie, Y., Wang, F., Wang, K., Yue, H., Lan, X., 2020. Responses of bacterial *phoD* gene abundance and diversity to crop rotation and feedbacks to phosphorus uptake in wheat. Appl. Soil Ecol. 154, 103604. https://doi.org/10.1016/j.apsoil.2020.103604.

Xiong, X., Wan, W., 2023. Distinct distribution patterns of rare and abundant alkaline phosphatase-harboring bacteria in plateau wetlands. Ecol. Indic. 146, 109803. https://doi.org/10.1016/j.ecolind.2022.109803.

Xu, L., Cao, H., Li, C., Wang, C., He, N., Hu, S., Yao, M., Wang, C., Wang, J., Zhou, S., Li, X., 2022. The importance of rare versus abundant *phoD*-harboring subcommunities in driving soil alkaline phosphatase activity and available P content in Chinese steppe ecosystems. Soil Biol. Biochem. 164, 108491. https://doi.org/10.1016/j.soilbio.2021.108491.

Yang, L., Du, L., Li, W., Wang, R., Guo, S., 2023. Divergent responses of *phoD*- and *pqqC*-harbouring bacterial communities across soil aggregates to long fertilization practices. Soil Till. Res. 228, 105634. https://doi.org/10.1016/j.still.2023.105634.

Yin, Y., Yang, C., Li, M., Yang, S., Tao, X., Zheng, Y., Wang, X., Chen, R., 2023. Biochar reduces bioavailability of phosphorus during swine manure composting: roles of phoD-harboring bacterial community. Sci. Total Environ. 858, 159926. https://doi.org/10.1016/j.scitotenv.2022.159926.

Zeng, X., Jiang, C., Huang, F., Li, J., Chen, Y., Wang, Q., Jin, Y., Liu, C., 2024. Stability and erodibility of aggregate affected by typical tree-herb ecosystems in karst area. Chin. J. Soil Sci. 55, 1565–1573. https://doi.org/10.19336/j.cnki.trtb.2024030403.

Zhang, X., Gao, G., Wu, Z., Wen, X., Zhong, H., Zhong, Z., Yang, C., Bian, F., Gai, X., 2020. Responses of soil nutrients and microbial communities to intercropping medicinal plants in moso bamboo plantations in subtropical China. Environ. Sci. Pollut. Res. Int 27, 2301–2310. https://doi.org/10.1007/s11356-019-06750-2.

Zhang, Z., Luo, R., Liu, Q., Qiang, W., Liang, J., Hou, E., Zhao, C., Pang, X., 2023. Linking soil phosphorus fractions to abiotic factors and the microbial community during subalpine secondary succession: implications for soil phosphorus availability. Catena 233, 107501. https://doi.org/10.1016/j.catena.2023.107501.

Zhu, M., Huang, B., Liu, Z., Wang, Y., Teng, J., Tian, X., Ai, X., Sheng, M., Ai, Y., 2022. The distribution, effectiveness and environmental threshold of soil aggregate phosphorus fractions in the sub-alpine region of Southwest China. Land Degrad. Dev. 34, 3–15. https://doi.org/10.1002/ldr.4401.